35th Annual International Conference of the IEEE EMBS
Osaka, Japan, 3 - 7 July, 2013

An Efficient Capacitive Sensing Scheme for an Ophthalmic Regional Anesthesia Training System

Biswarup Mukherjee[1], Boby George[1,2] *Member, IEEE* and Mohanasankar Sivaprakasam[1,2]
[1]Department of Electrical Engineering, Indian Institute of Technology Madras, India
[2]Healthcare Technology Innovation Centre, Indian Institute of Technology Madras, India
boby@ee.iitm.ac.in

***Abstract*— Ophthalmic regional blocks are critical preoperative procedures involving the insertion of a syringe needle into the orbital cavity at such a position and angle that akinesia and analgesia is achieved without damage or harm to the eye and its associated musculature. A training system that accurately represents the orbital anatomical features and provides qualitative feedback on the performed anesthetic technique, can be of immense help in reducing risks involved in regional block administration. In this paper, a training system that employs a special but simple capacitive sensing scheme has been developed. A rapid prototyped eye-model has been used to ensure anatomical accuracy. Capacitive transmitter electrodes placed on the orbital wall along the length of the extraocular muscles are excited with a special excitation sequence and the displacement current at the needle of the syringe is measured using simple electronic unit and a Data Acquisition System, enabling the developed Virtual Instrument to detect the depth of penetration and proximity of the syringe needle to the ocular muscles. Additionally, the system detects needle touch of the muscles accurately. The proposed electrode array system and excitation schemes have been validated on a prototype system thus demonstrating its usefulness for practical training purposes.**

I. Introduction

Administration of local anesthesia for ocular surgeries involves injecting the anesthetic fluid in the intra-orbital space. Complications such as retrobulbar hemorrhage, brain stem anesthesia and globe perforation have been widely reported [1]-[5] for all forms of practiced anesthetic techniques including peribulbar [3] and sub-Tenon's technique [5]. Fig. 1 illustrates a widely practiced regional blocking technique. It clearly shows how the position and angle of the needle along with the trajectory followed by it in the intra-orbital space is critical to avoid injury to the globe (eyeball) and its associated muscles or vasculature. Mastery of these techniques involves several hours of clinical training on human subjects or cadavers. Training on human subjects is extremely risky and is not advisable. Training on cadavers is ineffective since it is not possible to assess the damage caused due to a faulty blocking procedure. Therefore, a training system that can track the proximity of the syringe needle to important ocular structures and suitably evaluate the quality of the regional block will enhance the anesthetist's skills and reduce complication rates.

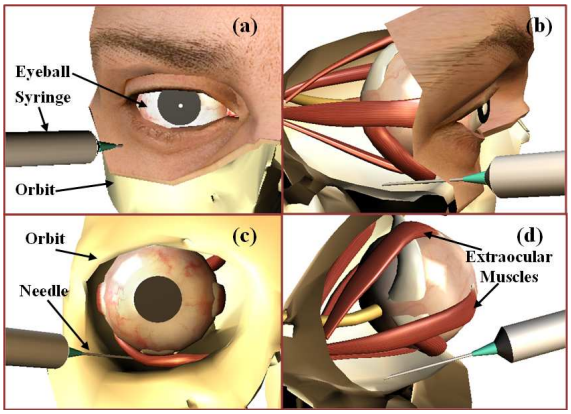

Fig. 1. (a) 3D model of eye showing the correct syringe insertion position and angle for a regional block. (b) Sagittal view of the orbit showing the needle penetration (c) Frontal view of the orbit showing the confined space for safe needle admission. (d) Posterior view of the orbital space showing the needle trajectory.

General anesthesia training manikins such as SimOne are not suitable for regional ophthalmic block training purposes [6]. The Ophthalmic Retrobulbar Injection Simulator (ORIS) is a virtual reality retrobulbar anesthesia simulator based on bulky and complex ultrasonic techniques to detect needle position [7]. It does not detect the proximity of the needle to ocular muscles. The capacitive array sensing based training manikin proposed in [8] lacks the underlying anatomical features of the eye and orbit necessary for accurate representation of the training environment. Haptic based simulators [9],[10] require complex finite element tissue deformation models, making them computationally burdensome and slow. Also, optical tracking systems used in [9] require direct line of sight between the imaging system and the needle, thus, restricting the movement of the trainee, who fails to perceive a true training environment.

In this work, we present a new training system for ophthalmic regional block techniques to overcome the challenges mentioned above. A capacitive electrode array and floating electrode based sensing and measurements scheme detects the proximity of the syringe needle to ocular muscles. The needle of the syringe acts as a measurement probe and the detected signal is fed to a LabVIEW based virtual instrument via appropriate signal conditioning circuits. A prototype developed validated the proposed capacitve scheme thus demonstrating its use for practical training purposes.

978-1-4577-0216-7/13/$26.00 ©2013 IEEE

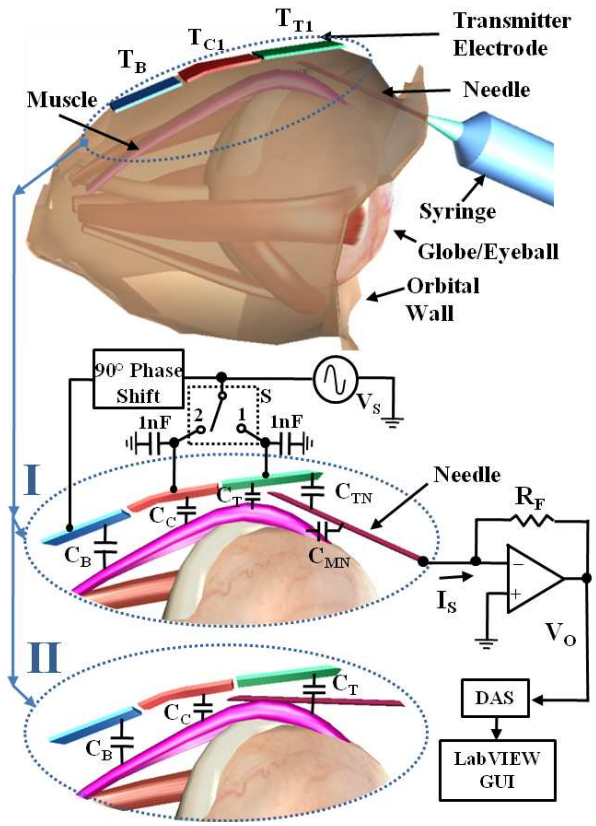

Fig. 2. A simplified diagram of the opthalmic regional block training system. The rapid prototyped 3D model of the globe and its associated muscles are shown. The electrode placement and the various capacitances formed between the electrode, muscle and the needle have been indicated.

II. Ophthalmic Regional Block Training System

Fig. 2 shows a simplified diagram of the regional block training system. The eye and its associated muscle structures are 3D printed. The muscles are coated with copper making them conductive, which forms the floating electrode of the sensing system. Connections are not drawn from the muscles thus rendering the eye-model freely removable from the orbit (eye-socket). The orbital wall that encloses the eye and its muscles, is lined with copper electrodes. Referring to Fig. 2, each muscle has 3 electrodes associated to it. The top electrode denoted by T_{T1} (Green) is directly above the anterior segment of the muscle (shown in pink), the central electrode denoted with T_{C1} (Red) covers the mid-section of the muscle and finally the base electrode, T_B covering the posterior segment of the muscle. T_{T1} and T_{C1} are connected to a 80kHz sinusoidal excitation source, V_S through a switch S. When not connected to V_S, T_{T1} and T_{C1} are pulled to ground potential (nearly) by 1nF capacitors. The base electrode, B, is always supplied by a 90° phase shifted version of the excitation signal, V_S.

The syringe needle is connected to an I-to-V converter with a shielded cable. The output, V_O of the I-to-V converter is fed to a Data Acquisition System (DAS) with a sampling rate of 500 kSa/s. The digital data is then processed by a Virtual instrument developed in LabVIEW. The VI employs a high-order Butterworth band-pass filter to admit only a very narrow band of frequencies centered around 80kHz, making it sensitive only to signals transmitted from the electrodes.

A. Capacitive Sensing Scheme

Fig. 2 shows the various capacitances that exist across the electrodes, muscle and the needle. The capacitances $C_T \approx C_B \approx C_C$, since the three electrodes are of the same dimensions and are almost equidistant from the muscle. When, the needle assumes a position as shown in I (refer Fig. 2) and switch S is in position 1, V_S is connected to T_{T1}. At the same time T_{C1} is pulled to ground. As the needle enters the space between the muscle and T_{T1}, capacitances C_{TN} and C_{MN} increase. As a result, I_S also increases in magnitude. Now, switch S is thrown to position 2, connecting V_S to T_{C1}. Since, T_{T1} is pulled to ground and the needle being at virtual ground, as an effect, C_{TN} is eliminated, and therefore I_S decreases as, $C_T \approx C_C$. Therefore, when the needle is close to T_{T1}, I_S increases when S is switched to 1 (T_{T1}) and I_S decreases when S is switched to 2 (T_{C1}). When, the needle touches the muscle (pink) as depicted in needle position II of Fig. 2 and switch S is thrown to position 1. The muscle being conductive forms an equipotential surface. Hence, V_O is given by (1),

$$V_O \approx R_F(\omega C_T V_S + \omega C_B V_S \angle 90°) \quad (1)$$

Hence, the magnitude and phase of V_O will depend on C_T and C_B. Since, $C_T \approx C_B$, then, $\angle V_O \approx 45°$ and $|V_O| \approx \sqrt{2} V_S \omega C_B R_F$. Since, $C_T, C_B >> C_{TN}, C_{MN}$, therefore, both, $|V_O|$ and $\angle V_0$ show a discrete jump when the muscle is touched by the needle. When S is switched to position 2, the magnitude and phase of V_O will depend on C_C and C_B and a similar large discrete jump in $|V_O|$ and $\angle V_0$ is exhibited. Thus, the event of the needle touching any of the muscle can be ascertained from the change in $|V_O|$ and $\angle V_0$.

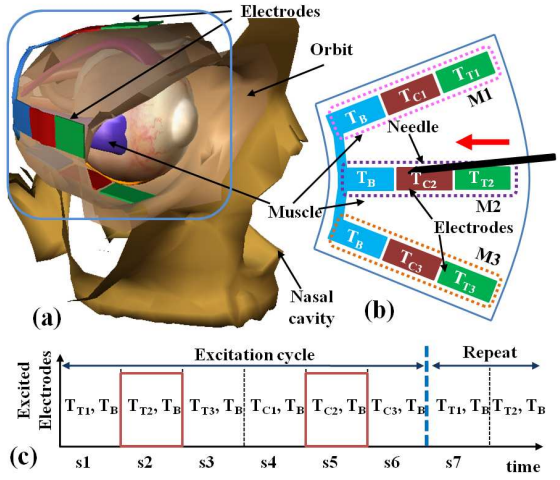

Fig. 3. (a) 3D view of the Top, Central and Base electrode placement inside the orbit for 3 muscles, $M1, M2$ and $M3$ (b) A planar simplified view of the electrode placement scheme. (c) Temporal excitation sequence followed to excite the various transmitter electrodes.

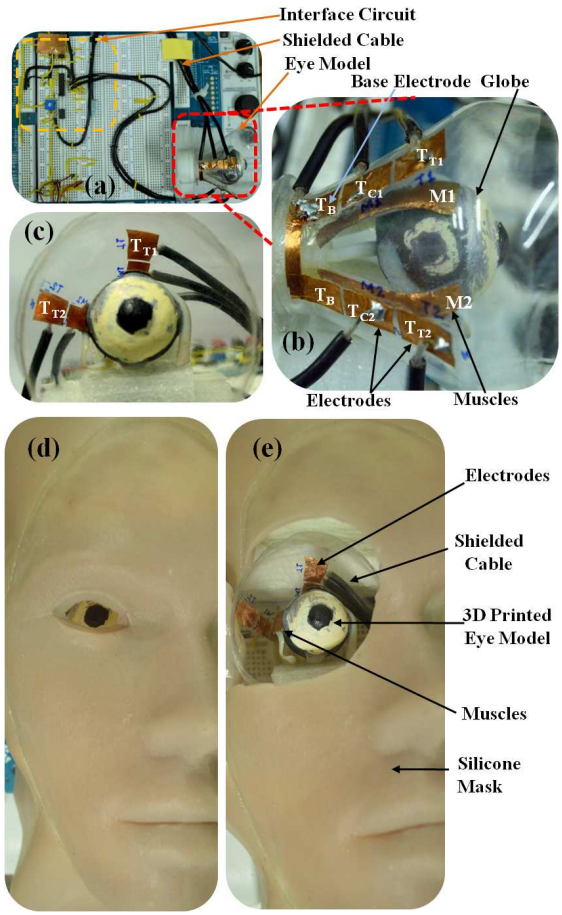

Fig. 4. (a) Top-View of the prototype system developed on a NI-ELVIS II platform (b) Close up view of the eye-model prototype showing the conductive muscle and its associated transmitter electrodes. (c) Front view of the eye-model (d) Top-View of the manikin based training system with silicone skin overlay. (e) Cut-away view of the manikin with the underlying eye-model and associated electrodes visible.

Fig. 3(a) shows the placement of the various electrodes corresponding to each muscle of the eye. A planar view of this electrode placement is shown in Fig. 3(b), along with the muscle overlap areas, denoted by M. The top electrodes, T_T and the central electrodes T_C are connected to the excitation signal V_S through a multiplexer. The base electrode is always supplied by a 90° phase shifted version of V_S as illustrated in Fig. 2.

Fig. 3(c) shows the temporal electrode excitation sequence followed in order to ascertain the depth of penetration of the syringe needle and the muscle being touched by the needle. Starting with T_{T1}, all the top electrodes, T_{T1}, T_{T2} and T_{T3} are excited one after the other, and V_O is recorded. This is followed by the excitation of central electrodes T_{C1}, T_{C2} and T_{C3} one after the other. Referring to Fig. 3(b), consider a case where the needle (shown in black) enters the orbit from outside, along muscle $M2$ in the direction specified by the red arrow. Now, as the needle enters the orbit, it passes between T_{T2} and $M2$. As a result, a change in $|V_O|$ and $\angle V_0$ is observed when T_{T2} is excited. As it enters further and passes between T_{C2} and $M2$, a similar change in $|V_O|$ and

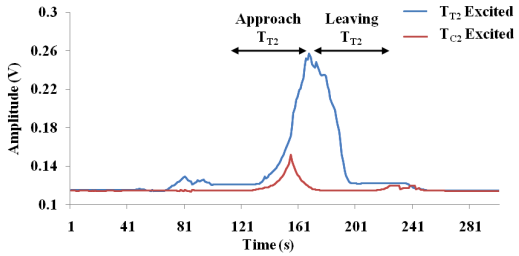

Fig. 5. $|V_O|$, when the needle is brought close to T_{T2} and then retreated back with T_{T2} excited and with T_{C2} excited.

$\angle V_0$ is observed when T_{C2} is excited. In all other excitations, no change in $|V_O|$ and $\angle V_0$ is observed. Therefore, from Fig. 3(c) it can be concluded that at time $s2$ the needle was in close proximity of T_{T2} and at time $s5$ the needle was in proximity of T_{C2}. Since, the switching rate is much faster than needle movement, hence, the depth of penetration of the needle can be detected in real-time. Additionally, if the muscle $M2$ is touched and if the depth of penetration is known and since, the switching frequency is high, it can be concluded that the depth at which the syringe needle has touched the muscle is same as the previously available depth of penetration of the needle . Hence, by adopting the electrode placement of Fig. 3(a) and (b) and the excitation sequence shown in Fig. 3(c), the depth of penetration and the depth at which muscle has been touched by the needle can be detected.

III. Results

A prototype system was developed to validate the practicality of the proposed capacitive sensing scheme. Fig. 4(a), shows an actual photo of the eye-model along with the associated signal conditioning and switching circuitry, implemented on a NI ELVIS II prototyping platform. Connections from the electrodes are drawn with shielded cables in order to reduce stray capacitance. Fig. 4(b) and (c) show a close-up orthographic and frontal view of the eye-model respectively with the Top, Central and Base transmitter electrodes marked. The muscles $M1$ and $M2$ have been made conductive by fixing copper strips on them. Connections are drawn from electrodes and not from the muscles directly. As can been seen, the prototype construction closely emulates the structure shown in Fig. 2 and Fig. 3. Fig. 4(d) shows the training manikin with a silicone skin overlaid to provide an accurate training environment for the trainee. Fig. 4(e) shows the underlying eye-model and the associated electrodes with the silicone skin layer cut-away.

Fig. 5 shows $|V_O|$ obtained from the developed prototype, when the needle is brought in the space between T_{T2} and then retreated back. It is observed that when T_{T2} is excited, as the needle approaches T_{T2}, $|V_O|$ rises and then decreases as it is retreated back from the orbit. No appreciable change in $|V_O|$ is observed when T_{C2} is excited. Therefore, the needle is detected to be close to $M2$ with depth of penetration as T_{T2}.

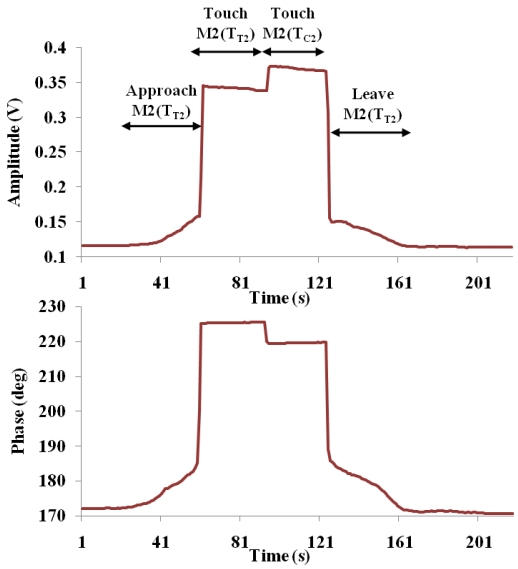

Fig. 6. $|V_O|$ and $\angle V_0$ when the needle is brought between T_{T2} and then muscle $M2$ is touched and finally retreated back. The various test conditions are shown and the excited electrode is indicated within parentheses

Fig. 6 shows readings obtained from the prototype for $|V_O|$ and $\angle V_0$ when the needle is brought between T_{T2} and $M2$ and then muscle $M2$ is touched and thereafter the needle is retreated back. It can be seen that with T_{T2} excited, as the needle approaches T_{T2}, $|V_O|$ and $\angle V_0$ starts increasing due to increase in C_{TN} and C_{MN} (refer Fig. 2). When, the muscle $M2$ is touched, a sharp rise in $|V_O|$ and $\angle V_0$ is observed as discussed in section II(A). Now, when the excitation is shifted to T_{C2}, the phase and amplitude show only slight variation. The $\Delta\angle V_0 \approx 45^\circ$ with respect to untouched condition, in both cases, indicating that $C_T \approx C_B \approx C_C$. As the needle is retreated with T_{T2} excited, a sharp fall in $|V_O|$ and $\angle V_0$ is observed which can be attributed to the release of needle touch from the surface of $M2$ and followed by a gradual decrease in $|V_O|$ and $\angle V_0$ as the needle is retreated from the space between $M2$ and T_{T2}.

From the tests conducted on the developed prototype system, it is found that the capacitive electrode placement scheme along with the excitation sequence proposed, is capable of detecting whether the needle of the syringe has touched a muscle and also the depth of penetration of the needle in the orbital space. This information is presented to the trainee thus providing feedback on the quality of the administered anesthetic procedure.

IV. Conclusion

A ophthalmic regional block training system based on a simple capacitive electrode array and excitation scheme was presented. A prototype was developed which consists of a 3D printed model of the orbit and eye with its associated appendages and is fitted with capacitive transmitter electrodes corresponding to muscles. The electrodes are excited with a special excitation sequence and the needle of the syringe acts as a measurement probe enabling a LabVIEW based Virtual Instrument to detect the depth of penetration of the needle and to determine whether a muscle is touched by the needle. No connections are drawn from the eyeball or the muscles making it freely removable from the eye-socket. Hence, the eye-ball can be easily replaced to emulate particular anatomical and pathological features as desired. Thus this system can serve an effective training system for ophthalmic regional anesthesia, thus improving the trainee's skill in administering regional blocks on live patients.

References

[1] H. Kallio, M. Paloheimo, and E. Maunuksela, "Haemorrhage and risk factors associated with retrobulbar/peribulbar block: a prospective study in 1383 patients." *Br J Ophthalmol*, vol. 85, pp. 708–711, 2000.

[2] R. Hamilton, "Brain-stem anesthesia as a complication of regional anesthesia for ophthalmic surgery." *Can J Ophthalmol*, vol. 27, pp. 323–325, 1992.

[3] W. Schrader, M. Schargus, E. Schneider, and T. Josifova, "Risks and sequelae of scleral perforation during peribulbar or retrobulbar anesthesia." *J Cataract Refract Surg.*, vol. 36, pp. 885–889, 2010.

[4] T. Eke and J. R. Thompson, "Serious complications of local anaesthesia for cataract surgery: a 1 year national survey in the united kingdom." *Br J Ophthalmol*, vol. 91, pp. 470–475, 2007.

[5] J. Frieman and M. A. Friedberg, "Globe perforation associated with subtenons anesthesia." *Am J Ophthalmol*, vol. 131, pp. 520–521, 2001.

[6] K. I. Hoffman and S. Abrahamson, "The cost-effectiveness of sim one," *J Medical Education*, vol. 50, pp. 1127–1128, 1975.

[7] J. R. Merril, N. F. Notaroberto, D. Laby, A. M. Rabinowitz, and T. E. Piemme, "The ophthalmic retrobulbar injection simulator (oris): an application of virtual reality to medical education," in *Proc Annu Symp Comput Appl Med Care.*, 1992, pp. 702–706.

[8] B. Mukherjee, B. George, M. Sivaprakasam, V. Jagadeesh Kumar, and J. Venkatakrishnan, "A capacitive array sensing based training system for ophthalmic anesthesia," in *Sensing Technology (ICST), 2011 Fifth International Conference on*, 28 2011-dec. 1 2011, pp. 623 –627.

[9] C. Sutherland, K. Hashtrudi-Zaad, P. Abolmaesumi, and P. Mousavi, "Towards an augmented ultrasound guided spinal needle insertion system," in *Engineering in Medicine and Biology Society,EMBC, 2011 Annual International Conference of the IEEE*, 30 2011-sept. 3 2011, pp. 3459 –3462.

[10] K. Naemura, A. Sakai, T. Hayashi, and H. Saito, "Epidural insertion simulator of higher insertion resistance & drop rate after puncture," in *Engineering in Medicine and Biology Society, 2008. EMBS 2008. 30th Annual International Conference of the IEEE*, aug. 2008, pp. 3249 –3252.